


# Optimization of a decellularization protocol of porcine tracheas. Long-term effects of cryopreservation. A histological study

The International Journal of Artificial  
Organs  
2021, Vol. 44(12) 998–1012  
© The Author(s) 2021  
Article reuse guidelines:  
sagepub.com/journals-permissions  
DOI: 10.1177/03913988211008912  
journals.sagepub.com/home/jao  


Lara Milian<sup>1,2</sup>, María Sancho-Tello<sup>1,2</sup>, Joan Roig-Soriano<sup>1</sup> ,  
Giovanna Foschini<sup>3</sup> , Néstor J Martínez-Hernández<sup>4</sup> ,  
Jorge Más-Estellés<sup>5</sup>, Amparo Ruiz-Sauri<sup>1,2</sup>, Javier Zurriaga<sup>1</sup>,  
Carmen Carda<sup>1,2,6</sup> and Manuel Mata<sup>1,2,7</sup> 

## Abstract

**Objective:** The aim of this study was to optimize a decellularization protocol in the trachea of *Sus scrofa domestica* (pig) as well as to study the effects of long-term cryopreservation on the extracellular matrix of decellularized tracheas.

**Methods:** Porcine tracheas were decellularized using Triton X-100, SDC, and SDS alone or in combination. The effect of these detergents on the extracellular matrix characteristics of decellularized porcine tracheas was evaluated at the histological, biomechanical, and biocompatibility level. Morphometric approaches were used to estimate the effect of detergents on the collagen and elastic fibers content as well as on the removal of chondrocytes from decellularized organs. Moreover, the long-term structural, ultrastructural, and biomechanical effect of cryopreservation of decellularized tracheas were also estimated.

**Results:** Two percent SDS was the most effective detergent tested concerning cell removal and preservation of the histological and biomechanical properties of the tracheal wall. However, long-term cryopreservation had no an appreciable effect on the structure, ultrastructure, and biomechanics of decellularized tracheal rings.

**Conclusion:** The results presented here reinforce the use of SDS as a valuable decellularizing agent for porcine tracheas. Furthermore, a cryogenic preservation protocol is described, which has minimal impact on the histological and biomechanical properties of decellularized porcine tracheas.

## Keywords

Decellularized tracheas, airway tissue engineering, SDS, cryopreservation, tracheal histology, tracheal stenosis

Date received: 26 January 2021; accepted: 17 March 2021

## Introduction

Different causes that affect the trachea, including malignant neoplasms, benign stenosis secondary to accidental trauma, or to congenital, inflammatory, or iatrogenic origin, lead to the resection of a circumferential segment of the trachea.<sup>1</sup> In these cases, end-to-end surgical anastomosis of the trachea is the gold standard. However, despite clinical successes, replacement of more than half of the trachea remains an unsolved challenge.<sup>2</sup>

In recent years, different alternative strategies have been followed in order to find a reliable tracheal substitute. A widely studied alternative includes the use of autologous tissues or organs, including skeletal muscle, esophagus, free

<sup>1</sup>Department of Pathology, Faculty of Medicine and Dentistry, Universitat de València, Valencia, Spain

<sup>2</sup>Research Foundation of the Clinical Hospital of the Comunidad Valenciana (INCLIVA), Valencia, Spain

<sup>3</sup>University Clinical Hospital of Valencia, Valencia, Spain

<sup>4</sup>Alzira Hospital, Valencia, Spain

<sup>5</sup>Biomaterials Center, Universitat Politècnica de València, València, Spain

<sup>6</sup>Center for Biomedical Research Network in Bioengineering, Biomaterials and Nanomedicine, Madrid, Spain

<sup>7</sup>Center for Biomedical Research Network of Respiratory Diseases, Madrid, Spain

## Corresponding author:

Manuel Mata, Department of Pathology, Faculty of Medicine and Dentistry, University of Valencia, Blasco Ibañez Avenue, 15, Valencia 46010, Spain.

Email: Manuel.mata@uv.es

periosteum, jejunum, bronchus, or aorta.<sup>1</sup> Unfortunately, limited success of these substitutes has been reported due to different causes, including biomechanics (mainly due to the absence of supporting cartilage and fibroelastic connective tissue), and a poor epithelialization which leads to impaired mucus clearance.<sup>1</sup> Tracheal allografts have also been considered by different researchers. Theoretically, they should be an ideal substitute because they contain a native respiratory epithelium and cartilaginous rings. However, important aspects related to revascularization, immunosuppression (which is not indicated for cancer patient), or preservation should also be considered.<sup>1</sup>

Decellularized tracheas represent another strategy for developing substitutes for tracheal replacement. Ideally, these scaffolds should be biomechanically compatible with the native trachea, as well as implantable in a feasible manner.<sup>3</sup>

Regarding the trachea, the strategies used for decellularization are heterogeneous and there is no a standard protocol. Virtually all protocols that remove cells from the different tissues conforming the tracheal architecture include the use of a non-ionic detergent. Among them, 4% sodium deoxycholate (SDC) in combination with DNase is the most commonly used.<sup>4–12</sup> Some authors have reported acceptable degrees of decellularization using other detergents such as sodium dodecyl sulfate (SDS), Triton X-100 or 3-((3-cholamidopropyl) dimethylammonio)-1-propanesulfonate (CHAPS) alone or in combination.<sup>13–20</sup> However, in many cases the authors have directly extrapolated the decellularization protocols reported in the literature, without considering important aspects such as differences in the composition of the extracellular matrix that exist between species.

A fast availability of decellularized tracheas is critical if we want to use them for clinical purposes. With this idea, different researchers have developed various strategies in order to minimize the decellularization time by including the use of enzymes that degrade the extracellular matrix such as trypsin, freezing and thawing, lyophilization, sonication, vacuum, or specific bioreactors in combination with detergents.<sup>13,16,18,20–22</sup> Another strategy developed to ensure the availability of decellularized tracheas when necessary is the cryogenic preservation of the tracheas once decellularized. Cryopreservation would not only allow a stock of organs ready for transplantation, but it also has other additional advantages. Long-term cryopreservation of tracheal grafts reduces antigenicity while preserving the biomechanical properties of the trachea in different animal models, including rats or pigs.<sup>1,23,24</sup> However, little is known about the morphology of decellularized cryopreserved tracheas, and, therefore, more detailed studies of the effects of cryopreservation on tracheas histology are needed.

The first objective of this study is to optimize a decellularization protocol in the trachea of *Sus scrofa domestica*

(pig). For this purpose, a preliminary study was carried out using detergents commonly used in the literature, including Triton X-100, SDS, and SDC. Then, a more detailed study was performed using an SDS concentration between 0.5% and 4%. Changes at the histological, biomechanical, and biocompatibility levels were evaluated in vitro. Our second objective is to study the effects of long-term cryopreservation on the extracellular matrix of decellularized tracheas, by histological and biomechanical methods.

We observed that, among the different detergents and concentrations tested, 2% SDS was the most efficient in removing chondrocytes while preserving histological organization of the tracheal structure. Long-term cryopreservation of decellularized trachea did not affect the biomechanical and histological properties of this organ. The results presented here reinforce the usefulness of SDS to obtain acellular tracheas, in addition to suggesting that cryopreservation is a suitable technology to preserve ready-to-implant decellularized tracheas.

## Materials and methods

### Study design

Porcine tracheas were dissected from the surrounding tissues and cut into 1.5 cm long rings. The tracheal rings were incubated in a mixture of phosphate buffered saline (PBS) and 5% antibiotics and antifungics, with different detergents, under continuous shaking for up to 4 weeks at room temperature (RT). For experiment (i), the following experimental groups were included (Table 1): (A) control group (not exposed to detergents), (B) 0.2% Triton X-100 + 0.25% SDS, (C) 2% Triton X-100 + 0.25% SDS, (D) 4% SDC, and (E) 2% SDS. Once a week, decellularization was evaluated by DAPI staining. After 4 weeks of treatment, the histological effects of the detergents were evaluated by optical microscopy, by using sections stained with hematoxylin eosin (HE), Masson's trichrome, Schiff's periodic acid (PAS), and orcein. DNA content was measured by spectroscopy. Six different tracheas were included in this study. All results were analyzed by comparing the decellularized rings with a control ring from the same animal. All stains were done at the same time to minimize the staining effect.

Next, a more detailed study was carried out to analyze the effect of SDS on the extracellular matrix of tracheas, since tracheas treated with SDS (E group) presented the best results. For experiment (ii), the tracheas were processed as indicated above, and the following experimental groups were included (Table 1): (A) control (not exposed to SDS), or exposed to different SDS concentrations: (F) 0.5% SDS, (G) 1% SDS, (E) 2% SDS, and (H) 4% SDS. The tracheas were incubated in PBS in the presence or absence of detergents for 4 weeks at RT with continuous shaking, as above. These samples were studied as in

**Table I.** Concentration (%) of the different detergents used in the experimental groups.

	Triton X-100 (%)	SDS (%)	SDC (%)
Experiment (i)			
Group A	—	—	—
Group B	0.2	0.25	—
Group C	2	0.25	—
Group D	—	—	4
Group E	—	2	—
Experiment (ii)			
Group A	—	—	—
Group F	—	0.5	—
Group G	—	1	—
Group E	—	2	—
Group H	—	4	—

experiment (i) (decellularization and optical microscopy), and also the ultrastructural organization of extracellular matrix was evaluated by scanning electron microscopy (SEM) in 2% SDS decellularized tracheas, as well as a morphometric study were carried out to analyze the effectiveness of chondrocyte removal and loss of fibers from the extracellular matrix. Six different tracheas were included in this study, and all results were analyzed by comparing the decellularized rings with a control ring from the same animal.

Since the samples treated with 2% SDS (E group) presented the best results once again, this group was further investigated through biomechanical and biocompatibility studies. The biomechanical properties of decellularized tracheas were evaluated in comparison with controls. The biocompatibility of the decellularized tracheas rings was tested *in vitro* by injecting human chondrocytes into the tracheal cartilage, and seeding human bronchial epithelial cells on the inner surface of the tracheal rings. Six different tracheas were included in this study. All comparisons were carried out by comparing a control ring with decellularized rings from the same animal, as expressed above.

To study the effects of cryopreservation on the composition of the extracellular matrix, tracheas decellularized with 2% SDS (group E) were frozen in liquid nitrogen and stored for up to 1 month. The biomechanical properties of frozen tracheal rings were compared to fresh rings from the same animal. The histological effects of cryopreservation were studied by optical microscopy and SEM as described above.

### Trachea decellularization procedure

Whole tracheas from Duroc pigs were kindly supplied by the slaughterhouse of Valencia (Mercavalencia, Valencia, Spain). Pigs weighing between 85 and 110 kg were slaughtered and tracheas were transported on ice to the laboratory facilities. The larynx, bronchi, and surrounding connective

tissue were removed, and the tracheas were washed three times with PBS supplemented with antibiotics. The tracheas were sectioned into 1.5 cm long rings and an osmotic shock was performed by incubating them in sterile distilled water for 2 h at RT. Between 6 and 8 rings were obtained from each trachea, depending of their length. As exposed above, the comparison between different treatments was made using rings from the same trachea to avoid interferences. After the osmotic shock, the tracheal rings were immersed in PBS containing penicillin/streptomycin and detergent, and incubated for up to 4 weeks at RT under continuous shaking at 300rpm using a PSU-10 orbital shaker (Biosan, Riga, Latvia). An osmotic shock was performed every 48h followed by three washes with sterile PBS, and then tracheal rings were immersed in fresh PBS with/without detergents. At the end of the process, an additional osmotic shock was performed and tracheal rings were immediately processed or cryopreserved for future determinations.

### 4',6-Diamidino-2-phenylindole (DAPI) nuclear staining

The decellularization process was evaluated weekly by DAPI staining. Small portions of tissue were obtained and embedded in Optimal Cutting Temperature (OCT) medium and the frozen samples were sectioned on a Leica CM1520 cryostat (Leica, Madrid, Spain). Slices of 8µm were obtained and, after three washes with milliQ water at RT to remove the OCT, they were stained with a DAPI solution (ThermoFisher Scientific, Madrid, Spain) following manufacturer's instructions. Preparations were visualized using a Leica DM 4000B inverted fluorescence microscope (Leica, Madrid, Spain).

### Histological and morphometric analysis

After the decellularization process, the tracheal rings reserved for histology were transversely divided in two halves. One of them was embedded in paraffin and stained for H-E, Masson's trichrome, or orcein. The other half was embedded in OCT and stained with PAS. Standard staining protocols were used. The composition of the extracellular matrix was evaluated in the stained samples using the Image Pro Plus 7.0 software (Media Cybernetics, Rockville, MD, USA). The samples were photographed at 40× magnification using a Leica DMD 108 microscope (Leica, Madrid, Spain). Five representative microphotographs of each of the tracheal layers were obtained, including mucosa, submucosa, cartilaginous layer, and adventitia. The relative content of collagen and elastic fibers was evaluated according to the percentage of areas stained with Masson's trichrome and with orcein, respectively, taking the mean value of the five sections of each sample, and then the mean value of the six samples

per experimental group, compared to the control one. The content of GAGs was studied in the same way in slices stained with PAS. For the study of cartilage decellularization, 10 different photographs were taken at 40× magnification of each trachea included in this study, using sections stained with Masson's trichrome. Chondral lacunae were classified according to three categories: non-decellularized (chondrocyte with intact cytoplasm and nucleus), partially decellularized (cellular debris inside the lacuna), and completely decellularized (empty lacuna). The percentages were calculated for each of the photographs analyzed.

### *DNA analysis*

Total DNA was isolated from tracheas using the DNA QIAamp Mini kit (Qiagen, Hilden, Germany) according to manufacturer's instructions. A fragment of 0.125 cm<sup>3</sup> was used from each trachea included in this study. DNA content was estimated by spectroscopy at 260 nm using a NanoDrop spectrophotometer (NanoDrop Technologies, Rockland, USA) and expressed as ng/mg of wet tissue.

### *Scanning electron microscopy (SEM)*

Ultrastructural analysis of the scaffolds, with or without seeded cells, was performed using a JSM-5410 scanning electron microscope (Jeol USA Inc., Peabody, MA, USA) as previously reported.<sup>25</sup> All samples were coated with a conductive layer of sputtered gold. An accelerating voltage of 20 kV was used to obtain micrographs.

### *Isolation and expansion of human chondrocytes*

Human primary chondrocytes were isolated from knee articular cartilage from donor patients who underwent total knee arthroplasty using standard protocols. All individuals provided their informed consent. The study was conducted in accordance with the Helsinki Declaration and applicable local regulatory requirements and laws. All procedures were approved by the Ethic Committee of the Hospital Clínico Universitario de Valencia (Spain). Chondrocytes were isolated using hyaluronidase, pronase, and collagenase as previously reported.<sup>25,26</sup> The resulting chondrocytes were cultured in chondrocyte proliferation culture medium (DMEM basal medium supplemented with 10% fetal bovine serum (FBS), 100 mg/ml ascorbic acid, 100 U penicillin, and 100 mg/ml streptomycin).

### *Culture of normal human bronchial epithelial (NHBE) cells*

NHBE cells were purchased from Lonza (Basel, Switzerland) and cultured in Bronchial Epithelial Cell

Growth Basal Medium (BEBM, Lonza, Basel, Switzerland) following manufacturer's instruction. Both chondrocytes and NHBE cell were cultured in a humidified atmosphere at 37°C and 5% CO<sub>2</sub>.

### *In vitro biocompatibility of scaffolds*

The biocompatibility of the decellularized group E scaffolds with living cells was studied considering both cell types: chondrocytes and bronchial epithelial cells. Isolated human articular chondrocytes ( $6 \times 10^6$  cells in 1 ml of chondrocyte culture medium) were injected into the wall of the decellularized tracheal rings using an insulin syringe, and chondrocyte-injected tracheal rings were cultured with chondrocyte culture medium for 1 week. Some tracheal rings were cut into 0.25 cm<sup>2</sup> fragments and normal human bronchial epithelial cells ( $3 \times 10^6$  cells in 1 ml NHBE cell culture medium) were seeded on the mucosal surface of decellularized tracheal fragments. Those NBHE cell-seeded tracheal fragments were completely covered with the BEBM culture medium and cultured for 1 week. DAPI staining was used to determine the nesting of both cell types.

### *Cryopreservation*

Whole tracheal rings were immersed in a cryogenic solution containing 20% DMSO in SBF, and frozen at a cooling rate of 1°C/min, using a freezing container (Nalgene® Mr. Frosty, Sigma-Aldrich, Madrid, Spain) with isopropanol, in a freezer at -80°C for 24 h. The samples were then stored in liquid nitrogen for at least 1 week and later processed for histological studies.

### *Biomechanical properties of decellularized tracheas*

The radial compression tests were carried out in a Microtest displacement-controlled UTS benchtop system (Microtest, Madrid, Spain), equipped with a 15 N load cell as previously described.<sup>5,6</sup> The Microtest SCM3000 95 software (Microtest, Madrid, Spain) was used for data collecting. The resolution of the measurements was 0.001 N for force, 0.001 mm for position, and 0.1 s for time. Data was collected every 0.5 s. The tolerated force,  $F(N)$  respect to the length of the specimen,  $L$  (mm) was calculated represented ( $F/L$ )

### *Analysis of results*

Data are shown as the mean  $\pm$  SEM of  $n=3-6$  different experiments. The statistical study was performed by analysis of variance (ANOVA) followed by the Turkey's multiple comparison test (GraphPad Software Inc., San Diego, CA). Significance was accepted at  $p < 0.05$ .

## Results

### Effectiveness of different combinations of detergents for the decellularization of porcine tracheas

Our first objective in this study was to optimize a protocol to decellularize porcine tracheas. During the decellularization process, the degree of decellularization was monitored weekly by DAPI staining. Nuclei removal was maximum at week 4. At this time point, specimens were fixed, processed histologically, and stained with hematoxylin eosin, Masson's trichrome, PAS, and orcein (Figures 1–4).

Histological examination of the control tracheas showed a structural organization similar to human. The mucosa layer consisted of a typical respiratory epithelium with predominance of ciliated and goblet cells and an underlying *lamina propria* over the submucosa layer composed of connective tissue (Figure 2, panel A). No physical structure was found to delimit the submucosal layer in which abundant muco-serous glands were found (Figure 2, panel B). Masson's trichrome staining revealed the presence of a loose connective tissue with abundant stromal cells and characteristic thin bundles of collagen fibers, which were more abundant in the submucosa than in the *lamina propria* (Figure 3, panels A and B). The cartilaginous layer was composed of a typical hyaline cartilage surrounded by a well-organized perichondrium (Figure 2, panels B and C). The presence of glycosaminoglycans (GAGs) was also observed in the entire connective matrix of the tracheal wall, defining characteristic chromatic areas in the cartilaginous layer, as evidenced by PAS staining, as well as highlighting the location of goblet and other mucous-secreting cells (Figure 4, panels A–C).

Representative panoramic images of pig tracheae before and after the decellularization process are shown in the Figure 1. As represented, none of the conditions altered the histological structure or organization of the cartilaginous layer of the trachea used.

All combinations of the detergents assayed completely removed the cells from the mucosa and submucosa layers (Figure 2, panels D, E, G, H, J, K, M, N). Regarding the cartilaginous layer, the detergents which achieved a greater chondrocyte removal were groups C (2% Triton X-100 + 0.25% SDS) (Figure 2, panel I) and E (2% SDS) (Figure 2, panel O), while tracheas of groups B (0.2% Triton X-100 + 0.25% SDS) and D (4% SDC), the degree of decellularization of the chondral layer was reduced (Figure 1, panels F and L). In general, all decellularized tracheas experienced a significant loss of collagen as evidenced by Masson's trichrome stain (Figure 3, panels D–O). This loss of collagen content was particularly relevant in the decellularized tracheas of the experimental groups C (2% Triton X-100 + 0.25% SDS) (Figure 3, panels G–I) and D (4% SDC) (Figure 3, panels K and L), while it was minimal in group B (0.2% Triton X-100 + 0.25

SDS) (Figure 3, panels D–F) and intermediate in group E (2% SDS) (Figure 3, panels M–O). A similar trend was observed for GAGs content, as summarized in Figure 4.

Next, the DNA content was measured in all groups included in experiment (i). DNA content in the control group A was  $5.21 \pm 0.252$  ng/mg tissue, which is a value statistically significant higher than DNA content in experimental groups C ( $0.18 \pm 0.021$  ng/mg), D ( $0.22 \pm 0.003$  ng/mg), and E ( $0.85 \pm 0.065$  ng/mg). DNA content in decellularized tracheas group B was of  $3.1 \pm 0.51$  ng/mg tissue, which is a statistically significant difference with respect to the rest of the experimental groups except the control one.

Finally, orcein staining was used to study the effects of decellularization on the composition of the elastic fibers of the tracheas. Only tracheas from group A (control) and decellularized tracheas from groups D (4% SDC) and E (2% SDS) were included in this study. In the control tracheas (group A), elastic fibers were abundant in all tracheal layers, but in the cartilaginous matrix (Figure 5, panel A). In the mucosa and submucosa layers, the elastic fibers showed a regular size and a precise arrangement. Just under the epithelium of the mucosa layer the elastic fibers were thin and with a predominantly concentric arrangement with respect to the lumen, while in the depth of the mucosa and in the submucosa layer, an alternation of circular and longitudinal arrangements of elastic fiber bundles with respect to the lumen was observed (Figure 5, panel B). In the adventitia layer, the content of elastic fibers was also relevant, with thinner fibers than in the mucosa and submucosa layer, and without a strict organization (Figure 5, panel C). The content and organization of elastic fibers were preserved in both experimental groups D and E, but no significant differences with respect to the controls were observed (Figure 5, panels D–I).

### Optimization of SDS concentration for decellularization protocol

Among all the detergents studied in experiment (i), 2% SDS (group E) showed the highest chondrocyte removal capacity with the least impact on the extracellular matrix. For this reason, an SDS concentration curve was used to determine the optimal percentage of such ionic agent, and SDS between 0.5% and 4% were tested in experiment (ii) (Table 1). During the decellularization process, tissue samples were taken at weeks 2 and 4, and DNA was extracted and measured by spectrophotometry. The results are represented in Figure 6, panel A. Only group E (2% SDS) was effective in tissue DNA clearance at week 2, when DNA removal was maximal. The rate of DNA removal was slower in all other experimental groups and none of them achieved satisfactory clearance levels.

Next, the effectiveness of SDS in removing chondrocytes from cartilage rings was evaluated. As described in the

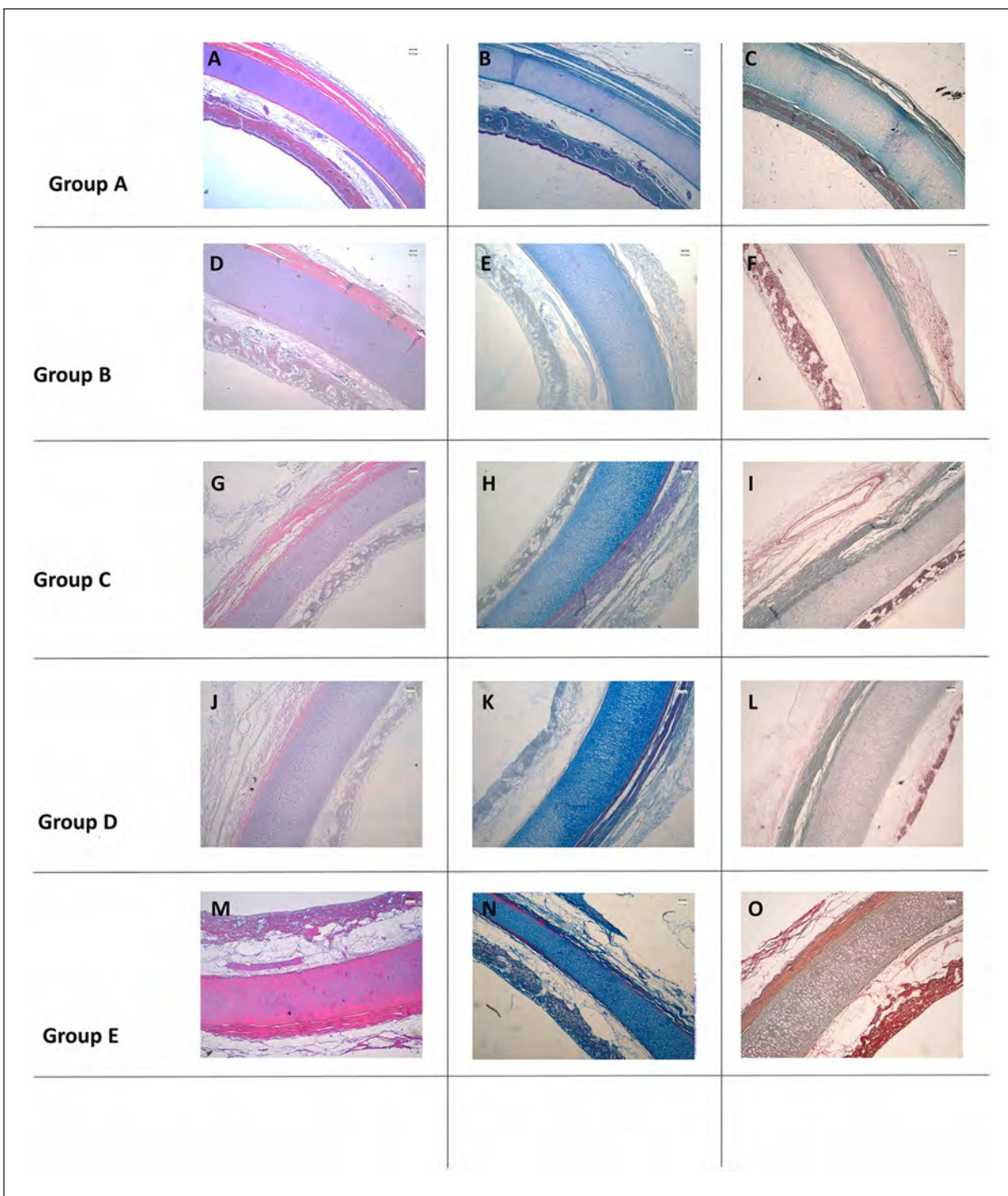


**Figure 1.** Panoramic view of porcine tracheas before and after decellularization. Porcine tracheas were cut in rings and incubated in the absence or presence of different detergents for up to 4 weeks. The following experimental groups were considered: A (non-exposed to detergents, control group, panels A–C), B (0.2% Triton X-100 + 0.25% SDS, panels D–F), C (2% Triton X-100 + 0.25% SDS, panels G–I), D (4% SDC, panels H–J), and E (2% SDS, panels K–M). The samples were processed and stained with hematoxylin eosin (panels A, D, G, J, and M), Masson's trichrome (panels B, E, H, K, and N), and orcein (panels C, F, I, L, and O). The results presented are representative of three different animals.

methods section, decellularized tracheas were stained with hematoxylin eosin and the number of non-decellularized, partially decellularized and completely decellularized lacunae was estimated. The results obtained are represented in

Figure 6, panel B. As it is shown, 2% SDS was the concentration of detergent that most efficiently eliminated the cells from lacunae, which was evident due to the limited number of intact chondrocytes detected.

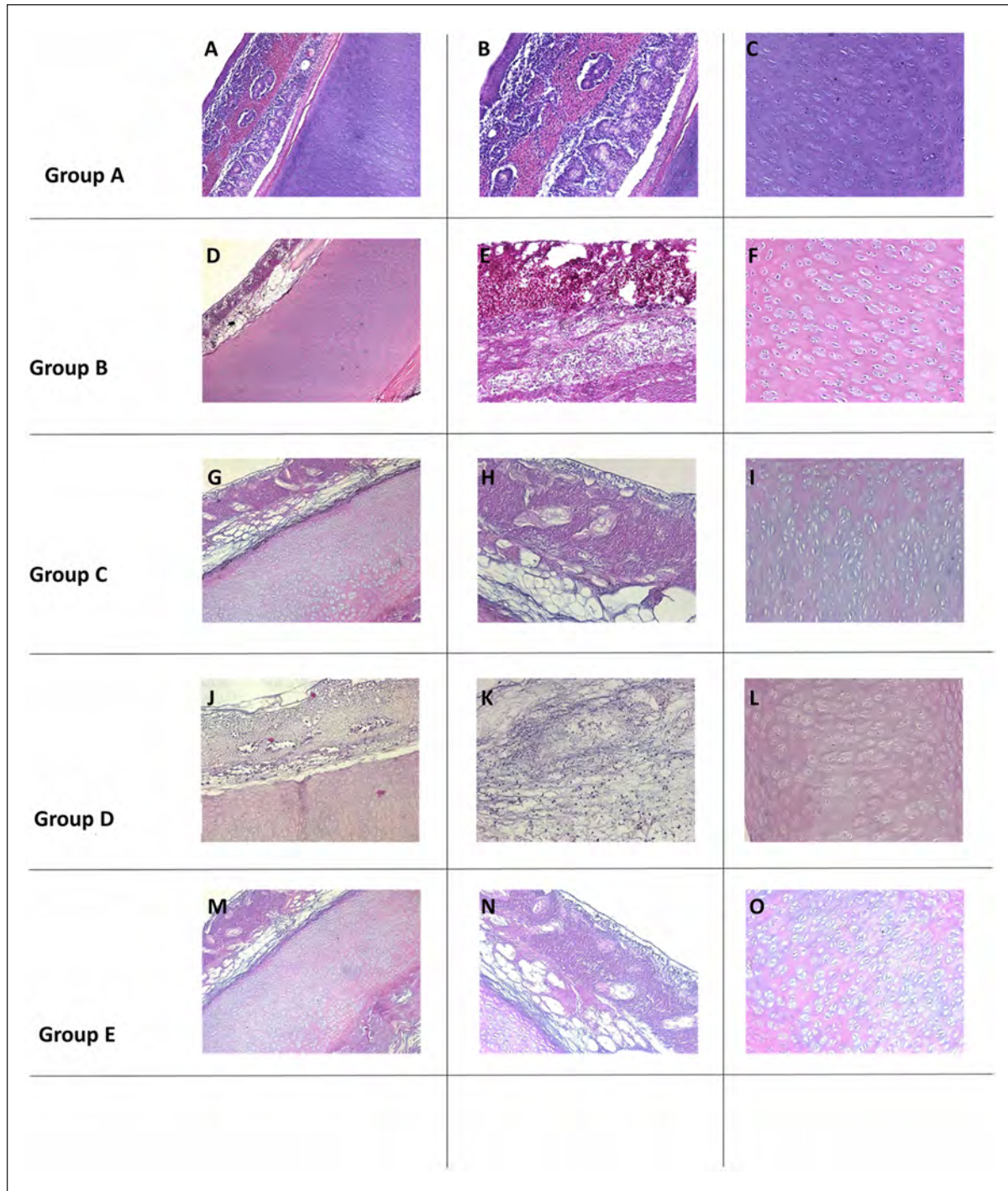


**Figure 2.** Hematoxylin eosin staining of decellularized porcine tracheas. Porcine tracheas were cut in rings and incubated in the absence or presence of different detergents for up to 4 weeks. The following experimental groups were considered: A (non-exposed to detergents, control group, panels A–C), B (0.2% Triton X-100 + 0.25% SDS, panels D–F), C (2% Triton X-100 + 0.25% SDS, panels G–I), D (4% SDC, panels H–J), and E (2% SDS, panels K–M). Samples were processed and staining with hematoxylin eosin. Representative panoramic (left column) and detail of mucosa (center column) and cartilage (right column) layers are shown. The results presented are representative of three different animals.

A morphometric analysis of the decellularized tracheas was carried out to study the effects of the different doses of SDS on the extracellular matrix composition. The samples

were stained with orcein. Then, the image J software was used to select collagen (blue stained) and elastic (red stained) fibers and the respective percentage of areas of each type of

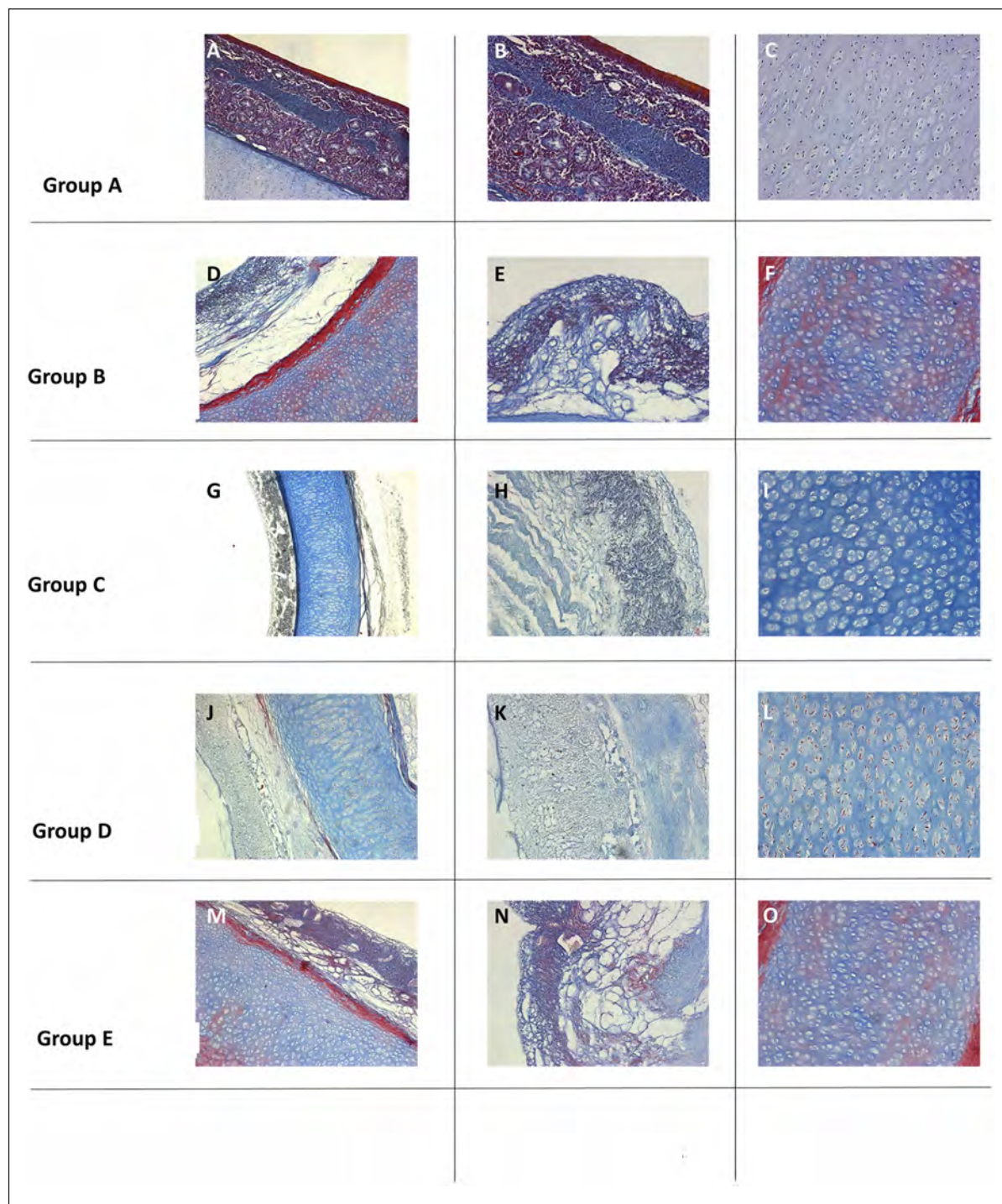


**Figure 3.** Masson's trichrome staining of decellularized porcine tracheas. Porcine tracheas were cut in rings and incubated in the absence or presence of different detergents for up to 4 weeks. The following experimental groups were considered: A (non-exposed to detergents, control group, panels A–C), B (0.2% Triton X-100 + 0.25% SDS, panels D–F), C (2% Triton X-100 + 0.25% SDS, panels G–I), D (4% SDC, panels H–J), and E (2% SDS, panels K–M). Samples were processed and staining with Masson's trichrome. Representative panoramic (left column) and detail of mucosa (center column) and cartilage (right column) layers are shown. The results presented are representative of three different animals.

fiber was calculated. The representative image of color mask selection is shown in Figure 6, panel C. In this example, the collagen fibers are yellow colored and the elastic fibers are red colored. As shown in Figure 6, panel D, none of the

concentrations tested affected the elastic fibers content. Regarding collagen fibers, the impact of all SDS concentrations was minimal, except for group E (2% SDS), which caused a loss of nearly 22% of the blue-stained area.



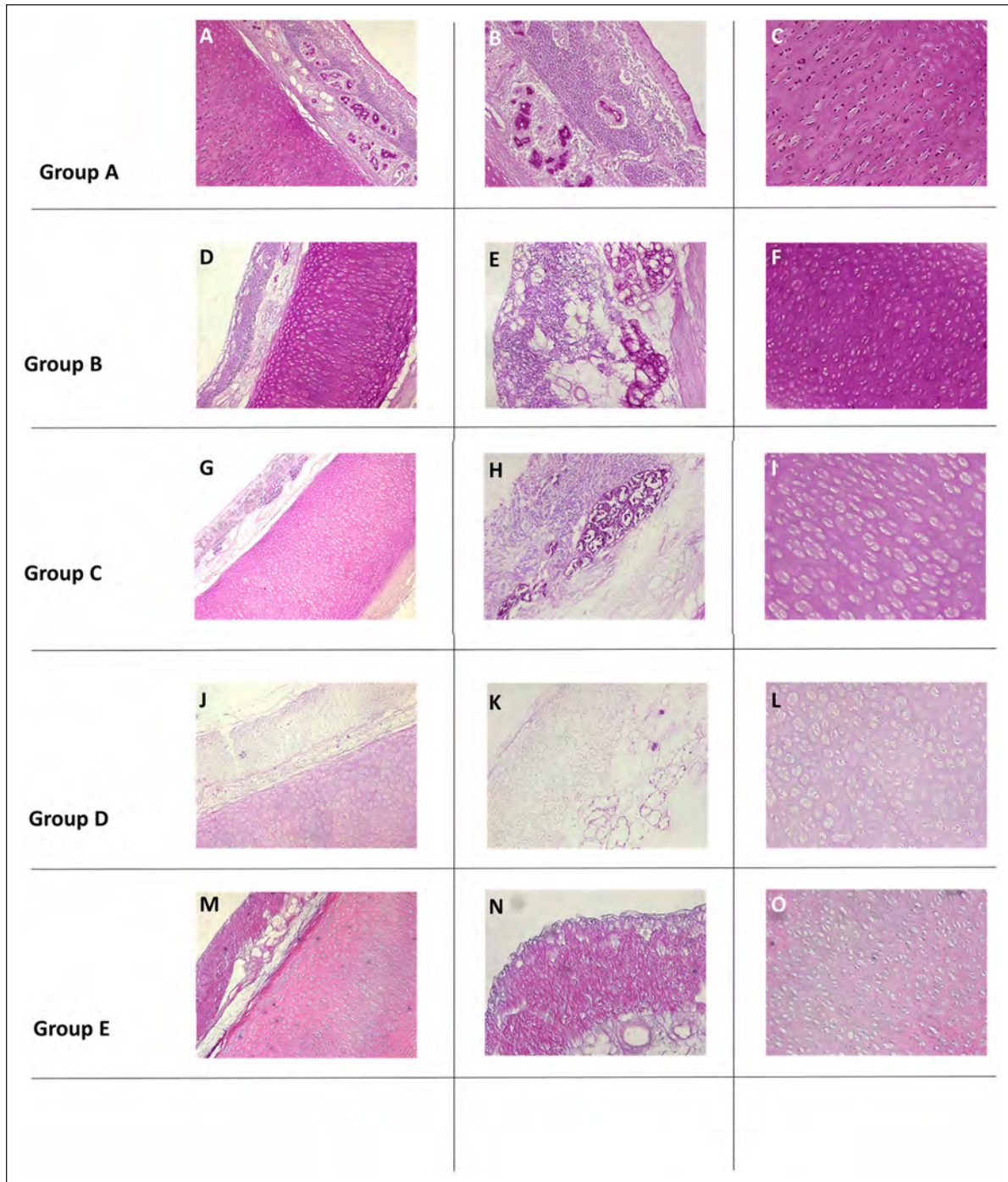


**Figure 4.** PAS staining of decellularized porcine tracheas. Porcine tracheas were cut in rings and incubated in the absence or presence of different detergents for up to 4 weeks. The following experimental groups were considered: A (non-exposed to detergents, control group, panels A–C), B (0.2% Triton X-100 + 0.25% SDS, panels D–F), C (2% Triton X-100 + 0.25% SDS, panels G–I), D (4% SDC, panels H–J), and E (2% SDS, panels K–M). Samples were processed and staining with PAS. Representative panoramic (left column) and detail of mucosa (center column) and cartilage (right column) layers are shown. The results presented are representative of three different animals.

#### *Biocompatibility of decellularized porcine tracheas*

Next, we decided to study whether decellularized tracheas were capable of promoting cell nesting *in vitro*, for both

chondrocytes and epithelial cells. The decellularized tracheal rings were immersed in chondrocyte proliferation culture medium and incubated at 37°C in the incubator. After 24h of culture, the medium was removed and chondrocytes were injected into the cartilage layer of the tracheal rings as

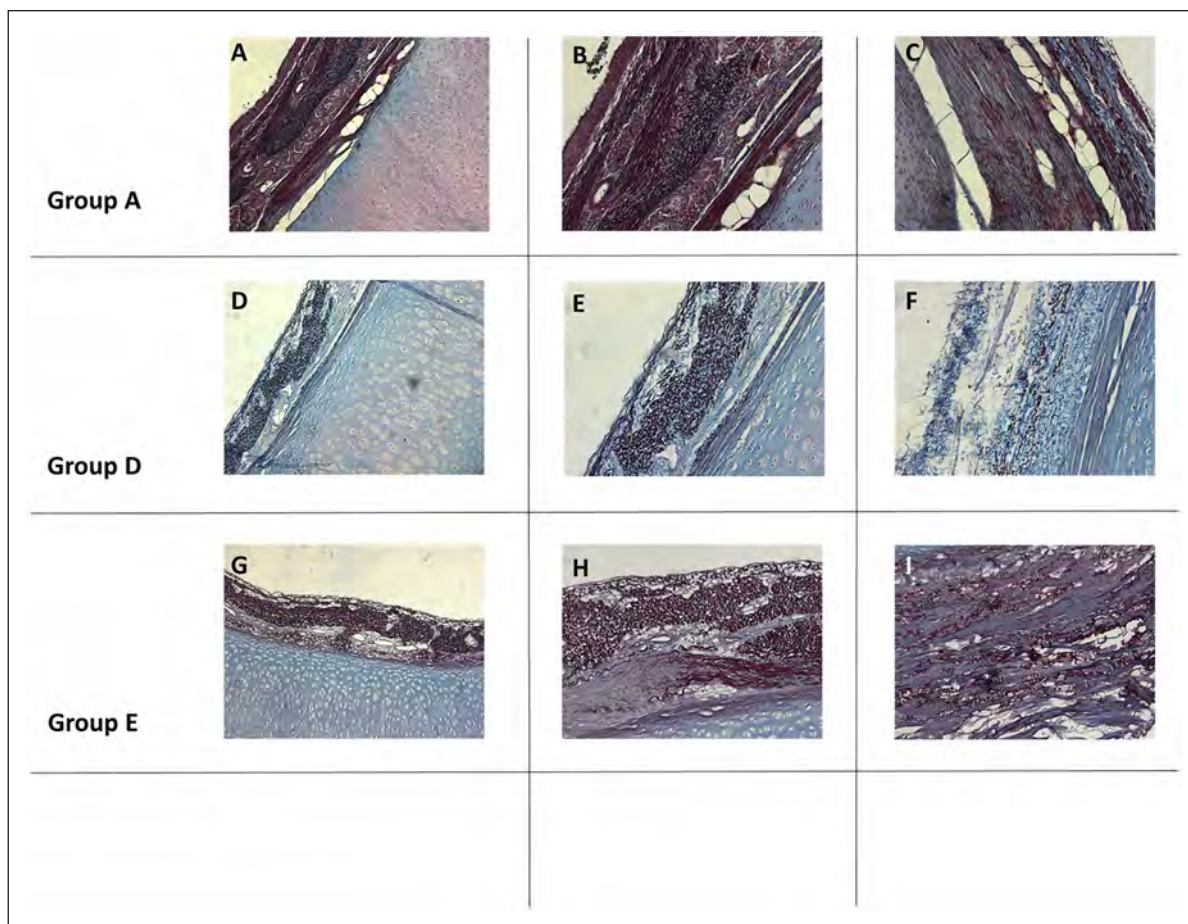


**Figure 5.** Orcein staining of decellularized porcine tracheas. Porcine tracheas were cut in rings and incubated in the absence or presence of different detergents for up to 4 weeks. The following experimental groups were considered: A (non-exposed to detergents, control group, panels A–C), D (4% SDC, panels D–F), and E (2% SDS, panels G–I). Samples were processed and staining with Orcein. Representative panoramic (left column) and detail of mucosa (center column) and adventitia (right column) layers are shown. The results presented are representative of three different animals.

detailed above. A representative image of the injection procedure is presented in Figure 6, panel E. Furthermore, some tracheal rings were sectioned into 0.25 cm<sup>2</sup> pieces, and used to seed NBHE cells on their mucosal surface. Both chondrocyte-injected and NBHE-seeded samples were cultured in their respective media and maintained for 1 week in the incubator. DAPI staining indicated the presence of cell nuclei in both the cartilaginous layer (Figure 6, panel F, showing the injected area of chondrocytes) and on the mucosa surface (Figure 6, panel G), in which some cellular mitosis could be observed (Figure 6, panel H). Regarding cartilage, the number of DAPI positive lacunae were significant higher in the injection areas than in the rest of the layer where the DAPI signal was minimal.

#### *Long-term cryopreservation of decellularized porcine tracheas*

The tracheal rings were decellularized using 2% SDS (group E), exposed to osmotic shock, and then cryopreserved. SEM analysis of the cryopreserved tracheas demonstrated

a normal distribution of connective fibers in the mucosa, submucosa, and cartilaginous layers, where chondral cell debris were observed in some of the lacunae (Figure 7, panel A). The morphometric study of histological processed tracheas showed no differences regarding the content of collagen and elastic fibers in frozen tracheas compared to the non-frozen tracheas (Figure 7, panel B).

Biomechanical analysis of 2% SDS decellularized tracheas (group E) from both fresh (non-frozen) and frozen samples was carried out as described in the methods section. All decellularized tracheas showed a significant decrease in *F/l* (Figure 7, panel C). Interestingly, a higher although not significant value of *F/l* was observed in the group of cryopreserved tracheas compared with to the non-cryopreserved decellularized experimental group.

#### **Discussion**

Tracheal stenosis represents a serious health problem with disastrous consequences on the quality of life of affected patients, in some cases leading to death. There is a current

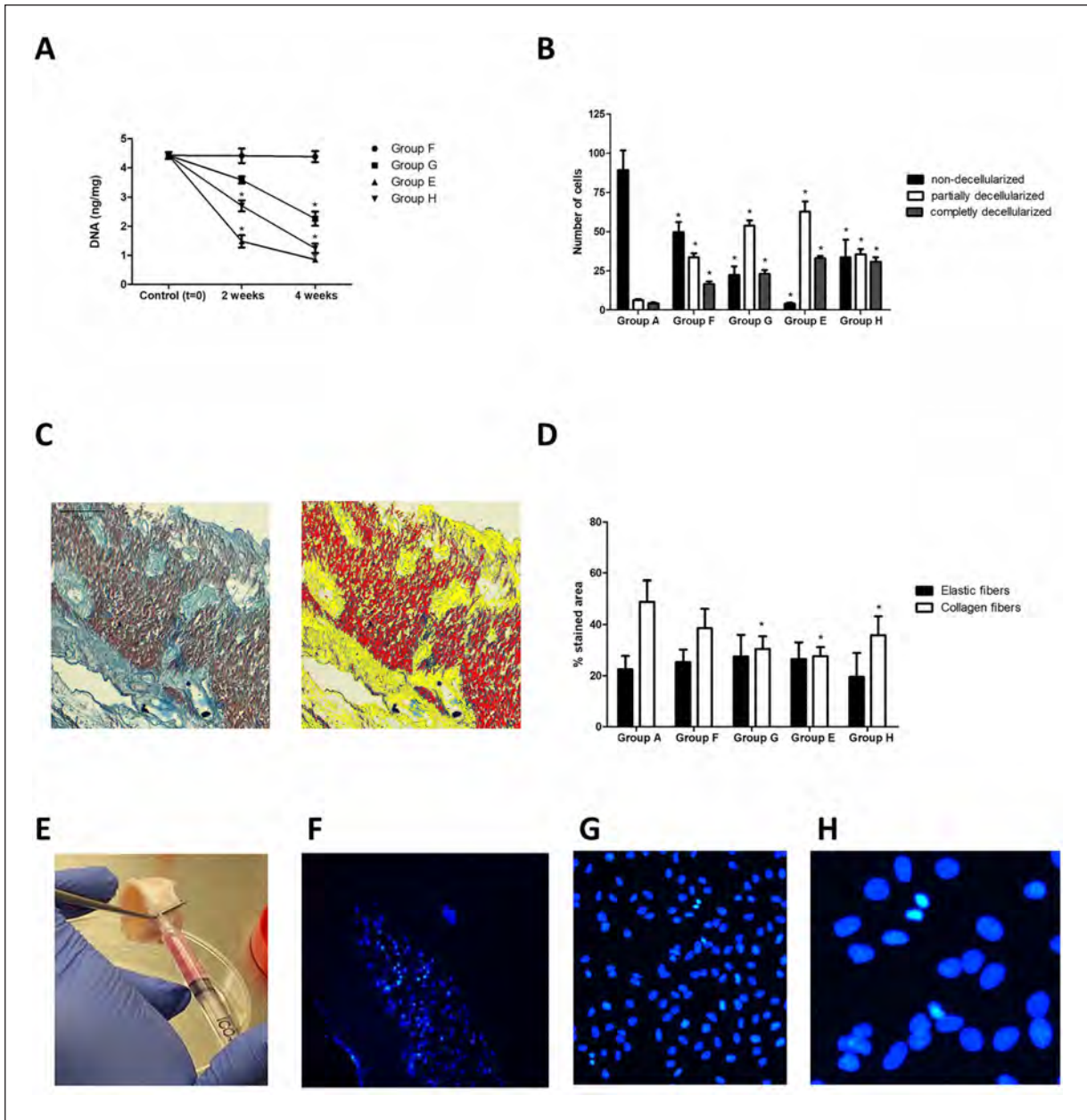


**Figure 6.** Panels A and B. DNA quantification and chondrocyte removal estimation of SDS decellularized porcine tracheas. Porcine tracheas were cut in rings and decellularized using 0.5%–4% SDS for up to 4 weeks. The following experimental groups were included: A (non-exposed to detergent, control group), F (0.5% SDS), G (1% SDS), E (2% SDS), and H (4% SDS). DNA content was estimated using a small portion of decellularized rings (panel A) at the following time-points: 0 (control), 2, and 4 weeks. The remaining tissue was staining with Masson’s trichrome and the number of non-decellularized (intact chondrocytes), partially decellularized (degraded chondrocytes), and completely (empty lacunae) decellularized was estimated (panel B). The results obtained are represented as mean ± SD in panel B. *n* = 3 different animals were used. \**p* < 0.05 compared to control group (group A). Panels C and D. Morphometric evaluation of collagen and elastic fibers in SDS decellularized porcine tracheas. The followings groups were included: A (non-exposed to detergent, control group), F (0.5% SDS), G (1% SDS), E (2% SDS), and H (4% SDS). The percentage of the area occupied by a blue staining (collagen fibers, yellow marked in the panel C) and red staining (elastic fibers, red marked in the panel D) was estimated using the Image J software. The results obtained are represented as mean ± SD in panel B. *n* = 3 different animals were used. \**p* < 0.05 compared to control group (group A). Panels E–H. Biocompatibility of decellularized porcine tracheas.  $6 \times 10^6$  chondrocytes in 1 ml of chondrocyte culture medium were injected in the cartilage layer (representative picture is shown in panel A), while in other rings,  $3 \times 10^6$  cells in 1 ml NHBE cell culture medium were seeded on the luminal surface of decellularized tracheal rings. Recellularized rings were cultured for 1 week and DAPI staining evaluated. Panel F: representative image of the chondrocyte injection area in the cartilaginous layer. Panel G: representative fluorescence image of the surface of the trachea. Panel H: detail of mitosis in the mucosal surface.

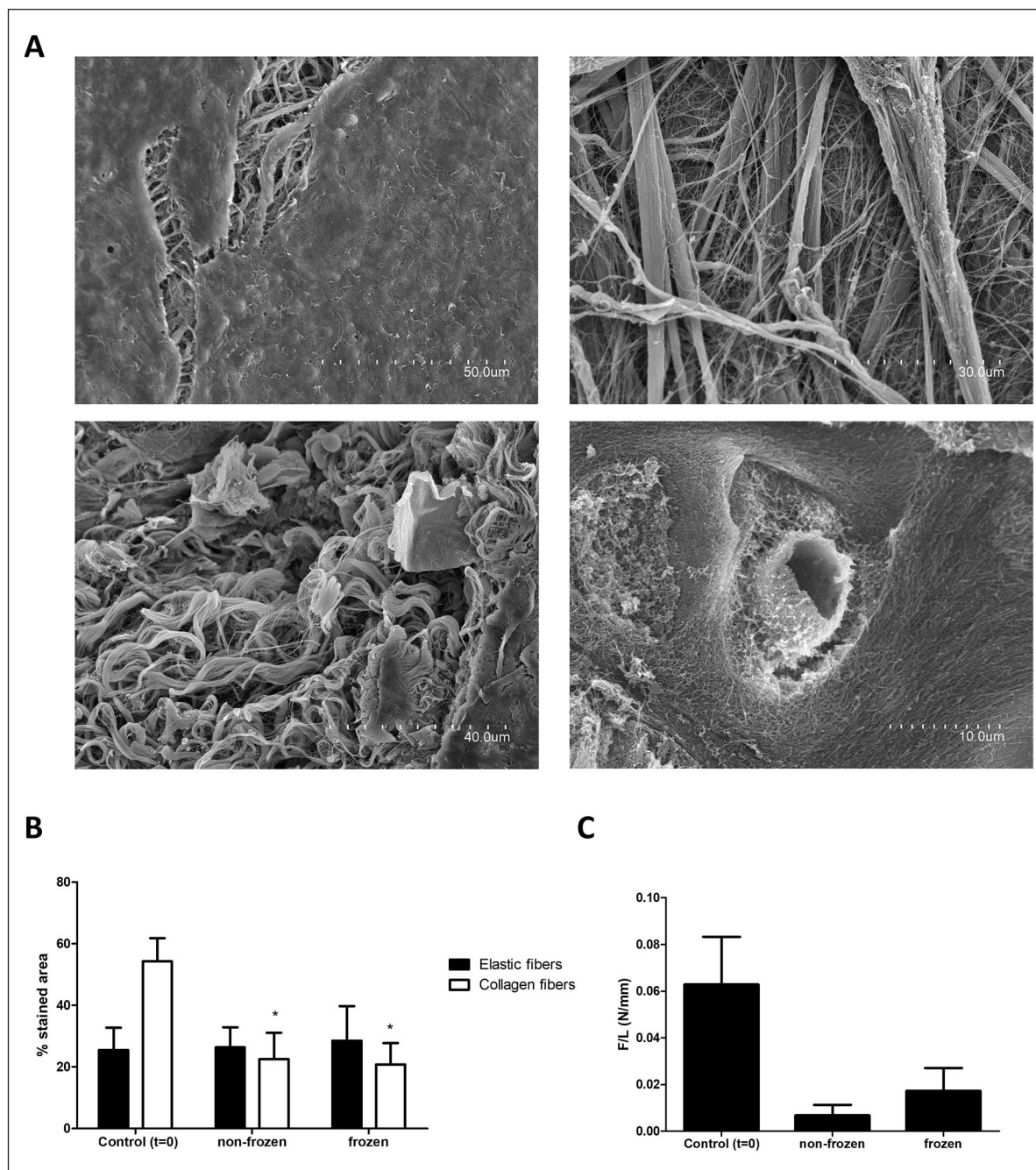


**Figure 7.** Histological and mechanical properties of long-term cryopreserved tracheas. Porcine tracheas were cut in rings and decellularized using 2% SDS for up to 4 weeks. The following experimental groups were included: control (non-decellularized tracheas), 2% SDS decellularized non-frozen tracheas and 2% SDS decellularized frozen tracheas. Representative images of SEM of basal lamina surface (panel A, up-left), lamina propria (panel A, up-right), submucosa (down-left) and cartilage (down-right) layers are shown in panel A. Panel B: morphometric analysis of processed tracheas stained with orcein. Panel C: Compression test of decellularized tracheas. The tolerated force,  $F(N)$  respect to the length of the specimen,  $L$  (mm) is represented ( $F/L$ ). Data presented are representative of three different animals. \* $p < 0.05$  compared to control group.

need for valid tracheal substitutes when more than 50% resection is performed. However, the complex biomechanics of the trachea is one of the factors responsible for the failure of different substitutes generated by tissue engineering techniques. For this reason, decellularized tracheal

matrix is a realistic source of compatible scaffolds, which could potentially be usefully for airway regeneration.<sup>16</sup> Complete removal of the cellular content of tracheas is necessary to avoid immunogenic responses that would lead to scaffold failure, especially because most candidate

patients are immersed in a carcinogenic process that precludes the use of immunosuppressants.<sup>27</sup> The removal of cells and cellular debris from the mucosa, submucosa, and adventitia layers of the trachea is not a problem as it is relatively simple, but things are different when it comes to the cartilaginous layer. In fact, some authors argue that it is impossible to completely decellularize the cartilaginous rings supporting the trachea.<sup>28</sup> Notwithstanding, the absence of vascularization of the hyaline cartilage represents an advantage, therefore a complete decellularization of the tracheal cartilage may not be necessary to avoid the immunological rejection of the scaffold.<sup>28</sup> This is an important aspect to consider because most decellularizing agents have a greater or lesser impact on the integrity of the extracellular matrix and an equilibrium must be reached between cell removal and the integrity of the supporting connective tissue. This balance should depend on the characteristics of the tracheal matrix, which are different in the diverse animal species and depends on aspects related to weight, size, neck length, or bipedal standing.<sup>29</sup>

Among the different decellularization agents, the use of ionic detergents, alone or in combination with physical methods, seems inevitable. Most reported decellularization protocols use SDC, generally at a 4% concentration, alone or in combination with other agents including non-ionic detergents such as SDS, CHAPS, or Triton X-100, enzymes such as trypsin, or physical agents that include vacuum or temperature, among others.<sup>13-20,22</sup> Nevertheless, in many investigations, the decellularization protocol used is not optimized for a particular animal species, or for other specific experimental conditions, and authors directly use 4% SDC. For this reason, our first objective was to optimize a specific protocol for the decellularization of porcine tracheas. We decided not to use complex equipment such as vacuum pumps or lasers to optimize an easily reproducible protocol in any conventional laboratory. All procedures were performed at RT and only an orbital shaker was used. We include some of the most widely used ionic detergents in the literature, alone or in combination. A group of animals treated with 4% SDC was included as a reference experimental group. We decide to include several osmotic shocks in the protocol, including one shock at the beginning of the protocol, another after each change of detergent solution, and a final shock at the end of the experiment. These osmotic shocks were added to increase the removal of cellular debris and DNA and detergent residues which could affect the viability of the generated decellularized matrix. Analysis of DAPI-stained samples indicates an optimal cell removal after 4 weeks of decellularization, and thus this was the time-point selected for the rest of the experiments. Taking in consideration our experimental conditions and the animal species selected, a fine histological analysis indicated that the samples treated with 2% SDS presented the best removal of cells from the tissue with the mild impact on

the composition and organization of the extracellular matrix. Interestingly, 4% SDS was less effective than 2% SDS in cell removal of processed tracheas. We attribute this effect to a considerable increase in the viscosity of the detergent solution due to its high concentration, which prevented the access of the detergent to the tissue. This effect could be minimized by using an incubator, but this would have involved the use of more instruments and this was out of our objectives. It is important to highlight that this conclusion is probably only valid for our experimental conditions and the animal species used, therefore a specific protocol should be optimized for other experimental variables.

Although SDS is a valuable decellularizing agent widely used in tissue engineering, it does not lack disadvantages, and in fact it has been reported that SDS can generate potentially cytotoxic residues that could affect the viability of the decellularized matrix.<sup>30</sup> In order to lessen this undesirable effect of SDS, we decided to include several osmotic shocks with distilled water to increase debris removal. Tracheas were first decellularized and then chondrocytes and NBHE cells were cultured in the cartilage layer or on the mucosal surface of decellularized tracheas, respectively, to test the effect of decellularization on cell viability. The results obtained indicated little deleterious effect on cell survival, as it was evidenced by the presence of intact nuclei and mitosis in both cartilage and mucosa layer of the tracheas.

An important aspect in regard to tracheal engineering is the need for ready-to-use substitutes, because affected patients cannot wait months for treatment and even, in a case of emergency, neither hours. Faced with this problem there are two possible solutions: shorten times for the decellularization procedure, or preserve the decellularized tracheas for future use. Several authors have improved the experimental procedures using strategies that include the use of negative pressure, decellularization cycles with different agents, the use of laser or different enzymes, etc. We propose that cryopreservation of tracheas could be a realistic solution for this problem, because it would allow a stock of ready-to-implant decellularized organs of different sizes. With this idea in mind, we present in this article a standardized protocol for cryopreservation of porcine decellularized tracheas with a long-term study of the evolution of the extracellular matrix organization and of the biomechanical properties of tracheas. Regarding histology, no effect has been observed for the cryopreservation of the trachea after 1 week compared to the non-cryopreserved. Regarding biomechanical studies, a moderate but not significant increase has been observed in some of the parameters analyzed. This observation agrees with other investigations and could be a consequence of the fact that freezing can induce changes in the characteristics of the proteoglycans of the extracellular matrix.<sup>31,32</sup> Nevertheless, the observed differences are minimal and not significant. It

is important to highlight that we have not study the biomechanical properties of each of the components of decellularized trachea, but of the whole trachea considered as a unit. Although studying the behavior of tracheal cartilage separately would be of interest, our aim was to obtain the most important clinically important information as described before.<sup>5,6,23</sup>

## Conclusion

In summary, the results presented here indicate that, on the one hand, the best decellularizing agent for porcine tracheas in our experimental conditions is 2% SDS and, in the other hand, the cryopreservation protocol used has no effect on the extracellular matrix composition and does not negatively influence the biomechanical properties of this acellular tracheal matrix. These results reinforce the need to optimize decellularization protocols based on the experimental model used, as well as demonstrate the usefulness of cryopreservation to have a stock of decellularized tracheas ready to use.

At this point we are ready to tackle the problem of vascularization of grafts, which is the true workhorse in tracheal tissue engineering.

## Acknowledgements

We sincerely thank to Teresa Sagrado Vives from the University of Valencia for her support with histological experiments. We are also grateful to the slaughterhouse of Valencia for supplying the samples that made possible this study.

## Declaration of conflicting interests

The author(s) declared no potential conflicts of interest with respect to the research, authorship, and/or publication of this article.

## Funding

The author(s) disclosed receipt of the following financial support for the research, authorship, and/or publication of this article: This work was supported by grants MAT2016-76039-C4-2-R (MST) and PID2019-106099RB-C42 (MM) from the Ministry of Economy and Competitiveness of the Spanish Government, by grant PI16-01315 from the ISCIII (Ministerio de Ciencia, Innovación y Universidades, Spain), and by grant PROMETEO/2020/069 (CC) from the local government of the Comunitat Valenciana (Spain), CIBER-BBN and CIBERER are funded by the VI National R&D&I Plan 2008–2011, Iniciativa Ingenio 2010, Consolider Program, CIBER Actions, and the Instituto de Salud Carlos III, with assistance from the European Regional Development Fund.

## ORCID iDs

Joan Roig-Soriano  <https://orcid.org/0000-0002-6134-3141>

Giovanna Foschini  <https://orcid.org/0000-0002-7131-3659>

Néstor J Martínez-Hernández  <https://orcid.org/0000-0002-5529-9615>

Manuel Mata  <https://orcid.org/0000-0002-1506-7983>

## References

1. Nakanishi R. Cryopreservation of the tracheal grafts: review and perspective. *Organogenesis* 2009; 5(3): 113–118.
2. Delaere P, Van Raemdonck D and Vranckx J. Tracheal transplantation. *Intensive Care Med* 2019; 45(3): 391–393.
3. Evaristo TE, CruzAlves FC, Moroz A, et al. Light-emitting diode effects on combined decellularization of tracheae. A novel approach to obtain biological scaffolds. *Acta Cir Bras* 2014; 29(8): 485–492.
4. Baiguera S, Del Gaudio C, Kuevda E, et al. Dynamic decellularization and cross-linking of rat tracheal matrix. *Biomaterials* 2014; 35(24): 6344–6350.
5. Butler CR, Hynds RE, Crowley C, et al. Vacuum-assisted decellularization: an accelerated protocol to generate tissue-engineered human tracheal scaffolds. *Biomaterials* 2017; 124: 95–105.
6. Johnson C, Sheshadri P, Ketchum JM, et al. In vitro characterization of design and compressive properties of 3D-biofabricated/decellularized hybrid grafts for tracheal tissue engineering. *J Mech Behav Biomed Mater* 2016; 59: 572–585.
7. Kiselevsky MV, Anisimova NY, Lebedinskaya OV, et al. Optimization of a method for preparation and repopulation of the tracheal matrix for allogenic transplantation. *Bull Exp Biol Med* 2011; 151(1): 107–113.
8. Partington L, Mordan NJ, Mason C, et al. Biochemical changes caused by decellularization may compromise mechanical integrity of tracheal scaffolds. *Acta Biomater* 2013; 9(2): 5251–5261.
9. Sun F, Pan S, Shi HC, et al. Structural integrity, immunogenicity and biomechanical evaluation of rabbit decellularized tracheal matrix. *J Biomed Mater Res A* 2015; 103(4): 1509–1519.
10. Tint D, Stabler CT, Hanifi A, et al. Spectroscopic analysis of human tracheal tissue during decellularization. *Otolaryngol Head Neck Surg* 2019; 160(2): 302–309.
11. Xu Y, Li D, Yin Z, et al. Tissue-engineered trachea regeneration using decellularized trachea matrix treated with laser micropore technique. *Acta Biomater* 2017; 58: 113–121.
12. Zang M, Zhang Q, Chang EI, et al. Decellularized tracheal matrix scaffold for tracheal tissue engineering: in vivo host response. *Plast Reconstr Surg* 2013; 132(4): 549e–559e.
13. Batioglu-Karaaltin A, Karaaltin MV, Ovali E, et al. In vivo tissue-engineered allogenic trachea transplantation in rabbits: a preliminary report. *Stem Cell Rev Rep* 2015; 11(2): 347–356.
14. Batioglu-Karaaltin A, Ovali E, Karaaltin MV, et al. Decellularization of trachea with combined techniques for tissue-engineered trachea transplantation. *Clin Exp Otorhinolaryngol* 2019; 12(1): 86–94.
15. Dimou Z, Michalopoulos E, Katsimpoulas M, et al. Evaluation of a decellularization protocol for the development of a decellularized tracheal scaffold. *Anticancer Res* 2019; 39(1): 145–150.
16. Giraldo-Gomez DM, García-López SJ, Tamay-de-Dios L, et al. Fast cyclical-decellularized trachea as a natural 3D scaffold for organ engineering. *Mater Sci Eng C Mater Biol Appl* 2019; 105: 110142.
17. Hong P, Bezuhly M, Graham ME, et al. Efficient decellularization of rabbit trachea to generate a tissue engineering

- scaffold biomatrix. *Int J Pediatr Otorhinolaryngol* 2018; 112: 67–74.
18. Lange P, Greco K, Partington L, et al. Pilot study of a novel vacuum-assisted method for decellularization of tracheae for clinical tissue engineering applications. *J Tissue Eng Regen Med* 2017; 11(3): 800–811.
  19. Urbano JJ, da Palma RK, de Lima FM, et al. Effects of two different decellularization routes on the mechanical properties of decellularized lungs. *PLoS One* 2017; 12(6): e0178696.
  20. Weymann A, Patil NP, Sabashnikov A, et al. Perfusion-decellularization of porcine lung and trachea for respiratory bioengineering. *Artif Organs* 2015; 39(12): 1024–1032.
  21. Guimaraes AB, Correia AT, Alves BP, et al. Evaluation of a physical-chemical protocol for porcine tracheal decellularization. *Transplant Proc* 2019; 51(5): 1611–1613.
  22. Hung SH, Su CH, Lin SE, et al. Preliminary experiences in trachea scaffold tissue engineering with segmental organ decellularization. *Laryngoscope* 2016; 126(11): 2520–2527.
  23. De Wolf J, Brieu M, Zawadzki C, et al. Successful immunosuppressant-free heterotopic transplantation of tracheal allografts in the pig. *Eur J Cardiothorac Surg* 2017; 52(2): 248–255.
  24. Liu Y, Zheng R, Ding J, et al. Histological examination of cryopreserved rat tracheal grafts. *ASAIO J* 2007; 53(4): 492–496.
  25. Sancho-Tello M, Martorell S, Mata Roig M, et al. Human platelet-rich plasma improves the nesting and differentiation of human chondrocytes cultured in stabilized porous chitosan scaffolds. *J Tissue Eng* 2017; 8: 2041731417697545.
  26. Martín-de-Llano JJ, Mata M, Peydró S, et al. Dentin tubule orientation determines odontoblastic differentiation in vitro: a morphological study. *PLoS One* 2019; 14(5): e0215780.
  27. Grillo HC. Development of tracheal surgery: a historical review. Part 2: treatment of tracheal diseases. *Ann Thorac Surg* 2003; 75(3): 1039–1047.
  28. Aoki FG, Varma R, Marin-Araujo AE, et al. De-epithelialization of porcine tracheal allografts as an approach for tracheal tissue engineering. *Sci Rep* 2019; 9: 12034.
  29. Dyce KM, Sack WO and Wensing CJG. *Textbook of veterinary anatomy*. 3rd ed. Philadelphia, PA: Saunders, 2002.
  30. Gilpin A and Yang Y. Decellularization strategies for regenerative medicine: from processing techniques to applications. *Biomed Res Int* 2017; 2017: 9831534.
  31. Lam SKL, Chan SCW, Leung VY, et al. The role of cryopreservation in the biomechanical properties of the intervertebral disc. *Eur Cell Mater* 2011; 22: 393–402.
  32. Theodoridis K, Müller J, Ramm R, et al. Effects of combined cryopreservation and decellularization on the biomechanical, structural and biochemical properties of porcine pulmonary heart valves. *Acta Biomater* 2016; 43: 71–77.